Electronic Supplementary Material (ESI) for Nanoscale Horizons.

Supplementary Materials for

Probing the mechanism of peroxiredoxin decamer interaction with its reductase sulfiredoxin from the single molecule to the solution scale

Audrey Beaussart*, Florent Canonico, Hortense Mazon, Jorge Hidalgo, Sarah Cianférani, Hélène Le Cordier, Alexandre Kriznik & Sophie Rahuel-Clermont*

*Corresponding authors. Email: sophie.rahuel@univ-lorraine.fr; audrey.beaussart@univ-lorraine.fr

This PDF file includes:

Materials and Methods
Supplementary references
Figs. S1 to S10
Table S1 and S2

MATERIALS AND METHODS

Production and purification of WT and mutant proteins. Recombinant *S. cerevisiae* wild-type and mutant Tsa1 fused or not with N-terminal His-tag were produced and purified following the experimental procedures previously described. [S1, S2] Final purification was achieved by gel filtration of the concentrated sample on a Superdex 200 column (GE Healthcare) equilibrated in a 50 mM Tris-HCl, 2 mM EDTA, 350 mM KCl pH 8.2 buffer. Wild-type and mutant Srx were produced and purified following the experimental procedures previously described, [S2] except cells were grown for 5 h at 37°C in LB medium containing ampicillin (200 $mg.L^{-1}$) supplemented by 0.5% glucose, followed by addition of 1:1 volume of cold LB medium containing 0.6% lactose, 20 mM HEPES pH 7.0, 1 mM IPTG and further incubation for 18 h at 20°C. Tsa1 and Srx mutants were generated by standard PCR site-directed mutagenesis and sequenced to confirm the presence of the desired mutation and that no mutations had been introduced in the amplification reactions. The identity and purity of Tsa1 and Srx proteins were confirmed by Coomassie stained SDS gel electrophoresis and by mass spectrometry analyses. Purified proteins were stored at -80°C in the presence of 10 mM DTT. Immediately before use, proteins were reduced by 10 mM TCEP for 30 min on ice, followed by desalting on a PD-10 MiniTrap G-25 column (GE Healthcare) equilibrated in 25 mM Na_2HPO_4, 100 mM KCl (PK) buffer pH 7.0. Protein monomer molar concentrations were determined spectrophotometrically using molar absorption coefficient at 280 nm of 29500 and 7280 $M^{-1}cm^{-1}$ for Tsa1 and Srx respectively. Preparation of $Tsa1_{SO2}$ was performed as previously described[S2] and of $Tsa1_{SS}$ by addition of 1.2 H_2O_2 equivalent to reduced Tsa1 in solution. Molar concentration of $Tsa1_{SO2}$ was determined [S2] using a molar absorption coefficient at 280 nm of 27500 $M^{-1}cm^{-1}$.

DLS analysis. DLS measurements were performed on a ZetaSizer Nano apparatus (Malvern Panalytical, Malvern, UK). Protein samples were pre-centrifuged for 1 h at 20 000 g at 4°C to eliminate particles with a hydrodynamic diameter greater than 1 µm that could interfere with the measure. $Tsa1_{SO2}$ concentration was fixed at 50 µM in the presence of increasing Srx concentrations from 0 to 500 µM in PK buffer pH 7.0. The hydrodynamic diameter of the samples was measured from an average of 25 runs for each Tsa1:Srx ratio (1:1, 1:2, 1:4 up to 1:50) using the Protein analysis mode of the DTS v4.2 software, and plotted *versus* the molar Tsa1:Srx ratio to obtain the titration curve.

Native mass spectrometry analysis. Prior to native MS experiments, the Tsa1 redox forms were desalted against 150 mM ammonium acetate buffer pH 6.9 using a PD-10 desalting column. The protein concentration was determined by UV absorbance. NanoESI-MS analyses were performed on an electrospray time-of-flight mass spectrometer (LCT, Waters, Manchester, UK) fitted with an automated chip-based nanoESI source (Triversa Nanomate, Advion, Ithaca, NY, USA). Acquisitions were performed in the positive ion mode after external calibration performed with the multiply charged ions produced by a 2-µM horse heart myoglobin solution diluted in water/acetonitrile/formic acid (50v/50v/1v). Tsa1 was diluted to 3 µM (in decamer) in a 150 mM

ammonium acetate buffer pH 6.9 and subsequently analyzed under carefully controlled parameters. The acceleration voltage applied on the sample cone (Vc) was set to 80 V or 120 V and the pressure in the first pumping stage of the mass spectrometer (Pi) was set to 6 mbar to achieve an efficient ion desolvation and transmission without disruption of non-covalent assemblies. Data analysis was performed with MassLynx 4.1 (Waters, Manchester, UK).

Fluorescence anisotropy titrations. The N-terminal amine of WT or mutant Srx was derivatized as previously described [S3] in 25 mM phosphate, 100 mM KCl buffer pH 8.0 by incubation with a ten-fold molar excess of the fluorophore Alexa Fluor 488 sulfodichlorophenol Ester (Molecular Probes, Life Technologies) for 30 min at room temperature in the dark. The labeled protein (AF-Srx) was separated from excess dye by a PD-10 MiniTrap G-25 column (GE Healthcare). The protein concentration and degree of labeling were determined by UV-spectroscopy, typically 30-60 %.

Fluorescence anisotropy titrations were carried out on a spectrofluorometer SAFAS Flx-Xenius equipped with dual monochromators as previously described [S3]. Briefly, the dissociation constant of the Tsa1/Srx complex was deduced from anisotropy titrations of 1 µM of AF-Srx with increasing concentration of Tsa1 in the PK buffer pH 7.0, recorded using 494 nm excitation and 528 nm emission wavelengths and 10 nm slits. Data obtained were expressed as the fraction of labeled protein in complex, taking into account the effect of complex formation on the fluorescence intensity. Plots of the fraction of AF-Srx in complex vs. Tsa1 concentration were fit to a single-site binding model to deduce the Tsa1/Srx dissociation constant. Dissociation constants are reported as the mean value ±standard deviation obtained from a minimum of n = 2 independent experiments performed on distinct protein productions.

Stopped-Flow Rapid Kinetics. The dilution-induced dissociation kinetics of the non-covalent Tsa1/Srx complex was monitored by Tsa1 intrinsic Trp fluorescence using a SX19MV-R stopped-flow apparatus (Applied Photophysics) equipped with a 20 µL cell, fitted for fluorescence measurements with excitation wavelength set at 295 nm and emitted light collected above 320 nm using a cutoff filter. One syringe contained Tsa1 (2.5 µM final concentration) and variable Srx (5 to 20 µM) mixture in PK buffer pH 7.0, and the other syringe contained the same buffer. The association kinetics were performed in similar conditions with Tsa1 (2.5 µM final concertation) in one syringe and Srx (5-50 µM) in the second syringe. Equal volumes of each syringe were rapidly mixed to induce dissociation and association, respectively. An average of at least six runs was recorded for each concentration of Srx. A control experiment was performed with Tsa1 alone. The data set obtained at variable Srx concentrations was fitted against multiexponential equation using SciDavis 1.2 software or analyzed by global fitting by the Kintek Explorer software using the model and equation described in Fig. S7.

Functionalization of AFM tips. AFM tips were functionalized with Srx (WT or L77R mutant) using PEG linker as previously described.[S3] Briefly, silicon nitride triangular-shaped cantilever with a nominal spring constant of 0.01 N/m (Bruker, MSCT-C) were washed in 5 ethanol and

chloroform baths, rinsed with ethanol, and dried with a stream of filtered N_2, cleaned for 20 min in a UV radiation and ozone cleaner (Novascan), then immersed overnight into an ethanolamine solution, washed 3 times in DMSO and 2 times with ethanol, then dried with N_2. The coated cantilevers were immersed for 2 h in Acetal-PEG-NHS solution dissolved in 0.5 mL chloroform with 10 µL trimethylamine (Sigma), then washed with chloroform and dried with N_2. Cantilevers were immersed for 10 min in citric acid (1%), rinsed with ultrapure water, and then capped with a 200 µL droplet of a PK buffer (pH 8.5 to favor N-terminal amine reaction) solution containing Srx (0.2 mg/mL, *i.e.* 14 µM) to which 2 µL of $NaCNBH_3$ solution were added. After 50 min, 5 µL of a 1 M ethanolamine solution was added to the protein droplet in order to inactivate unreacted aldehyde groups, and then washed and stored in PK buffer pH 7.0 at 4°C.

Preparation of Tsa1-coated surfaces. For Tsa1 decamer imaging, mica sheets were freshly cleaved using adhesive tape and covered with a 200 µL droplet of PK buffer pH 7.0 solution containing Tsa1 for 20 min, then rinsed 3 times with the same buffer. The optimal concentration to image a protein monolayer was found to be 100 nM.

For force spectroscopy measurements, the decamers were covalently attached to the support. For that, silicon wafers were coated by electron beam thermal evaporation with a 5 nm-thick Cr layer followed by a 30 nm-thick Au layer. Gold surfaces were washed in ethanol, dried with N_2, then exposed to a UV/O_3 cleaner for 20 min. The gold supports were then immersed in COOH-terminated thiols (16-mercaptohexadecanoic acid, Sigma) in ethanol overnight in the dark. The thiol-coated surfaces were rinsed with ethanol, dried with N_2, immersed in NHS/EDC solution (40 mg NHS/100 mg EDC in 4 mL of ultrapure water) for 30 min, then rinsed with ultrapure water. Finally, supports were covered with a 200 µL droplet of a PK buffer pH 7.0 solution containing Tsa1 for 1 h, then rinsed in the same buffer and immediately used for SMFS.

Atomic force microscopy imaging and single-molecule force spectroscopy (SMFS). AFM imaging was performed at room temperature (20°C) in PK buffer pH 7.0 supplemented with 2 mM TCEP, using a Dimension FastScan™ AFM from Bruker corporation (Santa Barbara, CA). Sharpened micro fabricated Si_3N_4 cantilevers (PEAKFORCE-HIRS-F-B with a nominal spring constant of 0.12 N/m from Bruker corporation) were used. Samples were imaged using PeakForce Tapping mode while keeping the applied force below 300 pN, using a frequency of 2 kHz and a 100 nm amplitude, at 512 lines per images.

To observe the Srx/Prx complex, a covalent complex linking Tsa1 and Srx catalytic Cys by a disulfide bond was first prepared *ex-situ*. The $Tsa1^{C171A}$ and $Srx^{C48A\ C106V}$ mutants, that retain the catalytic Cys as unique Cys residues were used to ensure the specificity of the reaction. $Tsa1^{C171A}$ was first activated in the PK buffer pH 7.0 for 15 min at 30°C by 2-pyridyldisulfide (2-PDS) in excess to generate the $Tsa1^{C171A}$-2-pyridine disulfide ($Tsa1^{C171A}$-SS-2TP) followed by desalting on a PD-10 MiniTrap 25-G. The $Tsa1^{C171A}$-SS-2TP concentration was calculated by measuring the absorbance at 280 nm, taking account of the contribution of the 2-pyridine thiol moiety, adding 5400 $M^{-1}cm^{-1}$ to the molar absorption coefficient of the protein. Srx was reacted with the $Tsa1^{C171A}$-SS-2TP at a 1:1 stoichiometry for 10 min at room temperature. Formation of the

$Tsa1^{C171A}$-SS-$Srx^{C48A\,C106V}$ (referred to as Tsa1-SS-Srx) was checked by SDS-PAGE analysis (Fig. S5). The complex (100 nM) was then deposited on freshly cleaved mica, rinsed and imaged in PK buffer pH 7.0.

SMFS was carried out at room temperature (20°C) in PK buffer pH 7.0, using a Dimension FastScan™ AFM from Bruker (Santa Barbara, CA) using the covalently attached Prx surfaces and Srx-decorated tips as described above, in PK buffer pH 7.0. Unless otherwise stated, all force curves were registered with an applied force of 250 pN, using a constant approach and retraction speed of 1 µm/s. Srx blocking experiments were performed by adding free Srx at a final concentration of 0.2 mg/mL (~14 µM) directly into the AFM chamber. All experiments were performed using untagged Tsa1, except experiments from Fig. 6 which used N-terminal His-tagged Tsa1 for comparison with His-tagged mutants. Control experiments performed with untagged $Tsa1_{SO2}$ and Srx confirmed that the His tag did not affect SMFS results. For S-S bond formation, the surface delay was switched from 250 ms to 1 s to promote S-S bond formation with a constant applied force of 250 pN and a constant approach and retraction speed of 1 µm/s. For S-S bond reduction, force curves were directly recorded after adding of TCEP reductant which was injected into the AFM chamber to obtain a final concentration of 2 or 4 mM.

Supporting Information references

S1 A. Kriznik, M. Libiad, H. Le Cordier, S. Boukhenouna, M. B. Toledano and S. Rahuel-Clermont, *ACS Catalysis*, **10**, 2020, 3326–3339.

S2 X. Roussel, G. Béchade, A. Kriznik, A. Van Dorsselaer, S. Sanglier-Cianferani, G. Branlant and S. Rahuel-Clermont, *J. Biol. Chem.*, 2008, **283**, 22371–22382.

S3 A. Bersweiler, B. D'Autréaux, H. Mazon, A. Kriznik, G. Belli, A. Delaunay-Moisan, M. B. Toledano and S. Rahuel-Clermont, *Nature Chemical Biology*, 2017, **13**, 909–915.

S4 P. Gouet, E. Courcelle, D. I. Stuart and F. Metoz, *Bioinformatics*, 1999, **15**, 305–8.

SUPPLEMENTARY FIGURES

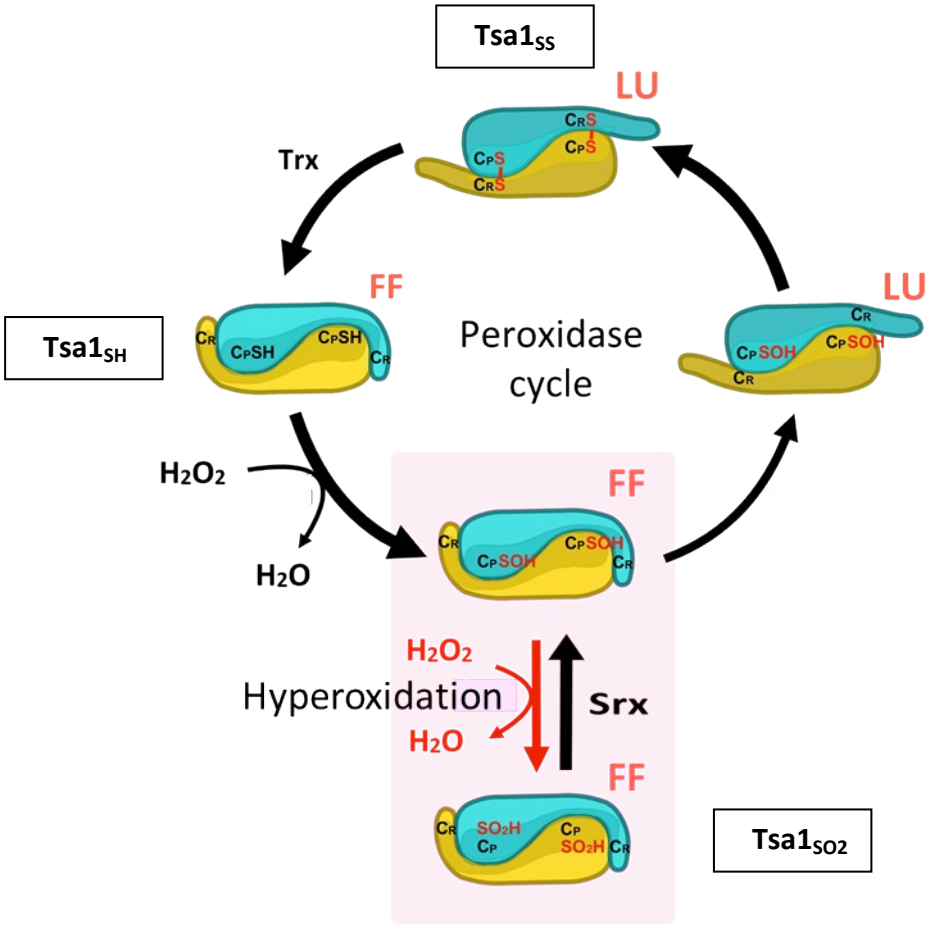

Fig. S1. The Prx catalytic and hyperoxidation cycles cycle shown at the level of the dimer.
The conformation of each subunit (blue and yellow) is indicated as FF (fully folded) and LU (locally unfolded). The local unfolding of each subunit C-terminal tail that includes the recycling Cys C_R, is schematized. The redox forms of Tsa1, *i.e* reduced $Tsa1_{SH}$, disulfide oxidized $Tsa1_{SS}$ and sulfinylated (hyperoxidized) $Tsa1_{SO2}$ are indicated. Trx : thioredoxin, C_P = Prx catalytic Cys. Adapted from [S1].

A

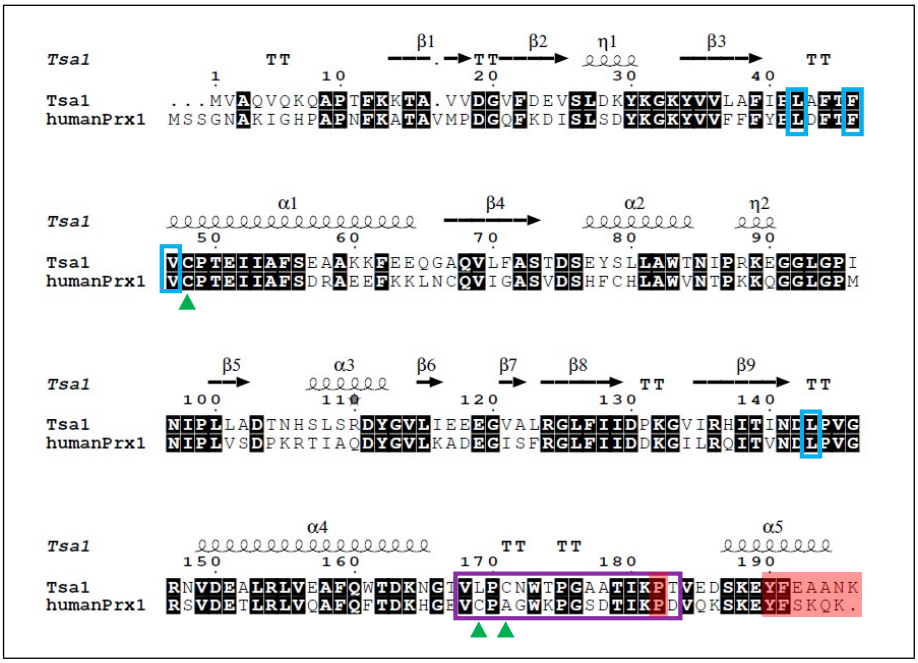

B

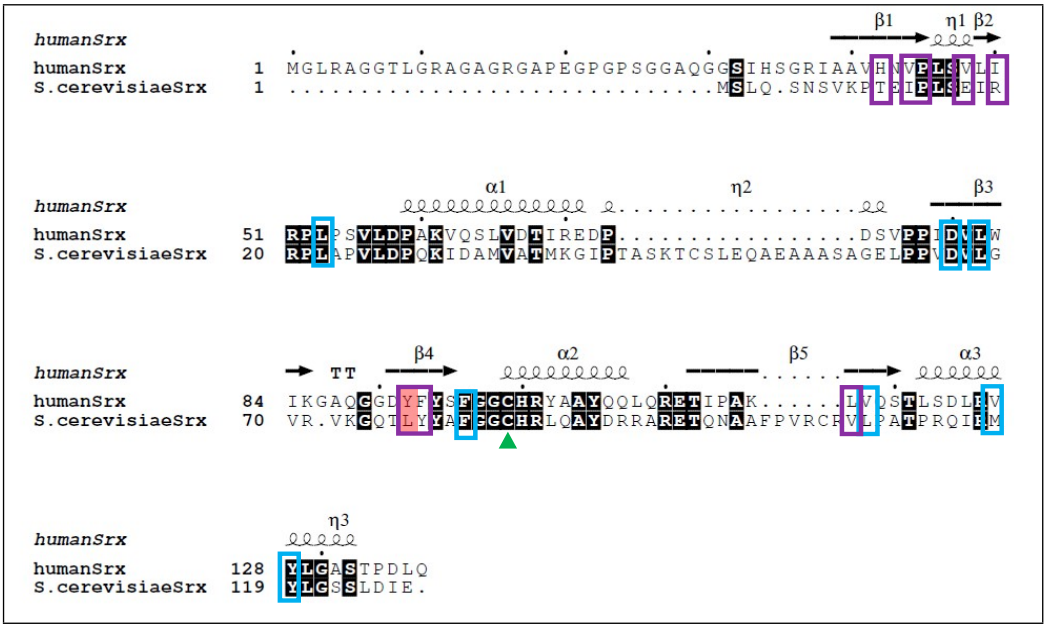

Fig. S2. Structure-based alignment of human and *S. cerevisiae* protein sequences.
(A) Comparison of Tsa1 and human Prx1 sequences. (B) comparison of Srx sequences. The secondary structural elements are shown above the alignments: α, α-helix; β, β-strand; η, 310 helix, TT, turn. Identical residues are on black background, residues from the active site interface in the human Prx1-SS-Srx complex are boxed in blue, from the backside interface in purple. Catalytic Cys in both proteins are indicated by a green arrow. The residues mutated in the study are on a red background. The alignment was built using the Espript server (http://espript.ibcp.fr [S4]).

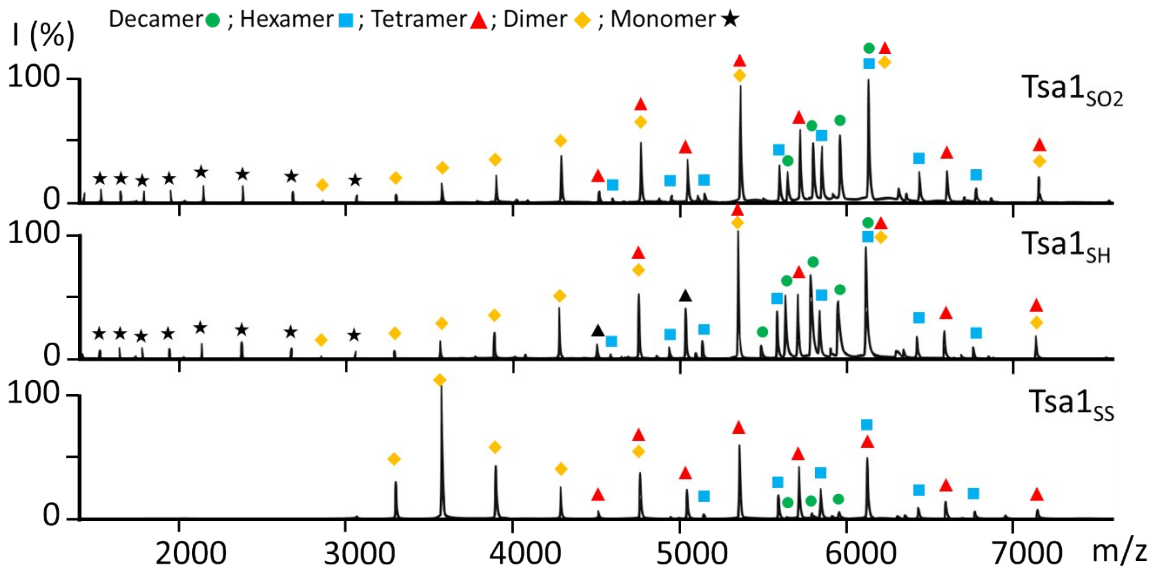

Fig. S3. Electrospray ionization mass spectra of Tsa1 redox forms ($Tsa1_{SO2}$, $Tsa1_{SH}$ and $Tsa1_{SS}$) obtained in native conditions (3 µM in decamer) showing the dissociation of the decamer (●; 215 kDa) into hexamers (🕘; 129 kDa), tetramers (①; 86 kDa), dimers (🕘; 43 kDa) and monomers (★; 21.5 kDa) in the gas phase at voltage Vc=120 V.

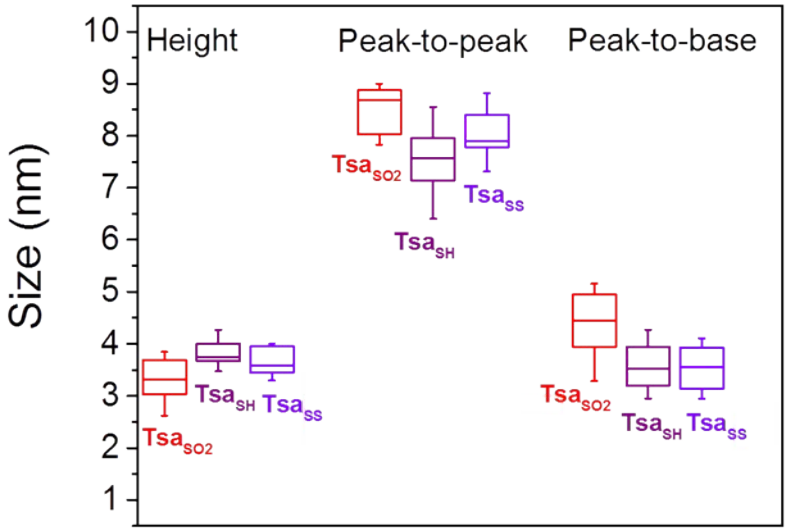

Fig. S4. Statistical dispersion of Tsa1$_{SO2}$, Tsa1$_{SH}$ and Tsa1$_{SS}$ decamers dimensions (height, peak-to-peak and peak-to-base as indicated on the sections in Fig. 3F), shown by box charts.

The bottom and top of the boxes represent the 25th and 75th percentiles, and the whiskers the 10th and 90th percentiles. The horizontal bands represent the median. Data in the box plots stem from measurements taken on at least 25 donuts for each Tsa1 redox forms.

A

$Tsa1^{C171A}{}_{SH}$ + 2PDS → $Tsa1^{C171A}$ -SS-2TP + 2TP

$Tsa1^{C171A}$ -SS-2TP + $Srx^{C48AC106V}$ → $Tsa1^{C171A}$ -SS-$Srx^{C48AC106V}$ (Tsa1-SS-Srx)

B

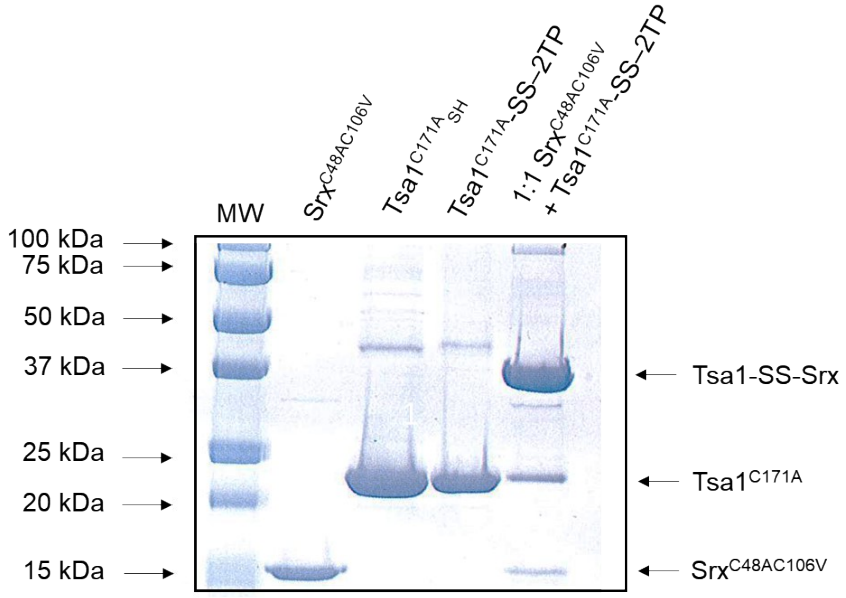

Fig. S5. (A) Principle for the preparation of the covalent Tsa1-SS-Srx complex. (B) Validation of the preparation of the Tsa1-SS-Srx complex by SDS-PAGE under denaturing non-reducing conditions.

After activation of $Tsa1^{C171A}{}_{SH}$ Cys C_P by 2-pyridyldisulfide (2PDS), yielding the $Tsa1^{C171A}$-SS-2TP mixed disulfide with a pyridine 2-thiol (2TP) moiety, reaction with the catalytic Cys of $Srx^{C48AC106V}$ (1:1 monomer:monomer) leads to near complete formation of the Tsa1-SS-Srx mixed disulfide with a molecular weight (MW) of 37 kDa. In solution under non-denaturing conditions, the complex exists as a $(Tsa1\text{-}SS\text{-}Srx)_{10}$ decamer. Additional bands on the gel correspond to minor secondary oxidized Tsa1 or Srx species.

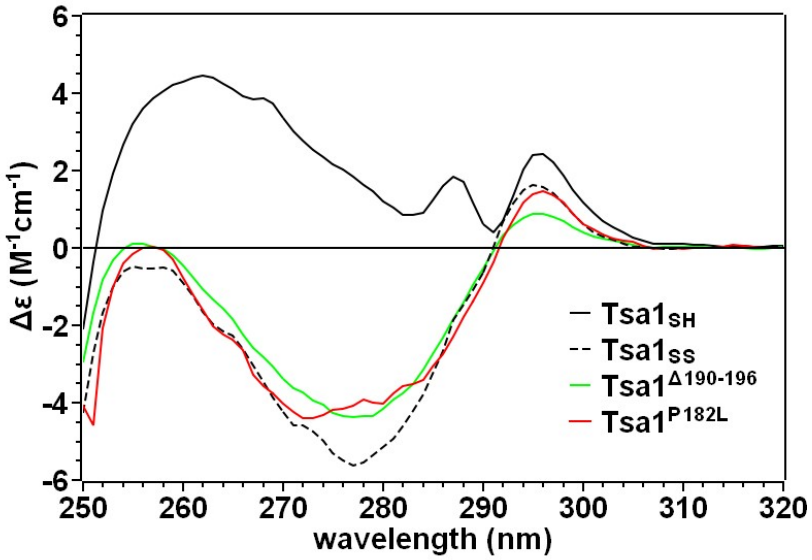

Fig. S6. Near-UV circular dichroism spectra of wild-type and mutant Tsa1.

Near-UV circular dichroism spectra of 50 μM Δ190-196 (green) and P182L (red) Tsa1 mutants under the reduced state, compared to wild-type Tsa1 (black) under the reduced (plain) and disulfide forms (dash). Measurements were performed in a 1 cm cuvette in phosphate 10 mM, NaF 100 mM buffer pH 7 and are the average of three records.

A

(1) Tsa1 + Srx ⇌ Tsa1•Srx k_1, k_{-1} forward and reverse rate constants, respectively

(2) Tsa1•Srx ⇌ Tsa1•Srx* k_2, k_{-2} forward and reverse rate constants, respectively

$$Fluo\ (V) = p * [\text{Tsa1•Srx}] + q * [\text{Tsa1•Srx}^*] + offset$$

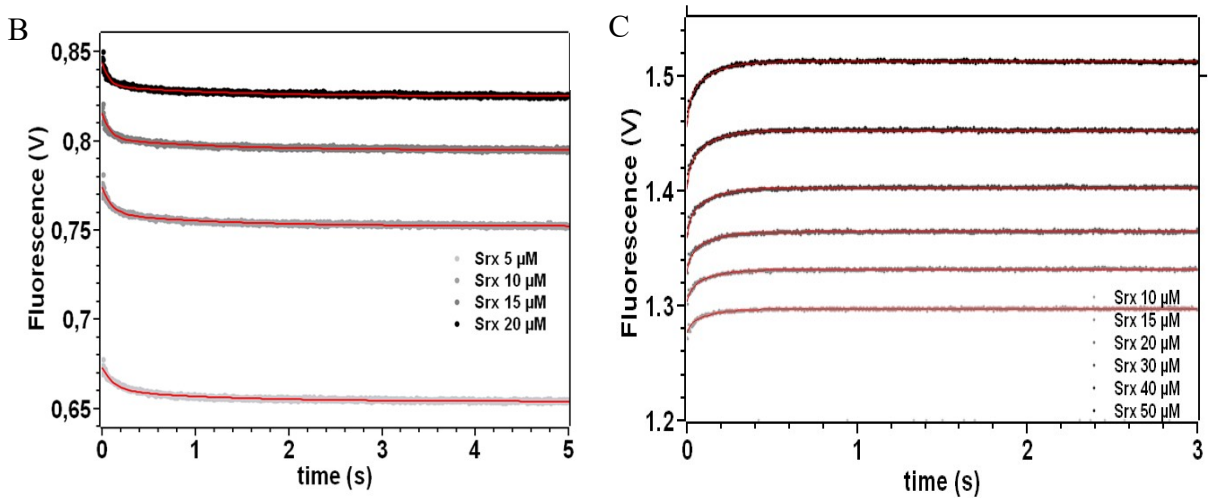

Fig. S7. Dissociation kinetics of the Tsa1/Srx complex in solution monitored by Trp fluorescence-based rapid kinetics.

(A) Two-step model and equation used to adjust the kinetic data: (1) second-order dissociation step, (2) first-order conformational reorganization step within the Tsa1•Srx complex, leading to the Tsa1•Srx* complex. The p and q parameters represent fluorescence intensity factors accounting for variation of the signal between free Tsa1 and Tsa1•Srx and Tsa1•Srx* complexes, respectively. *S. cerevisiae* Srx does not contain any Trp residue and thus only contributes to background signal. The offset fluorescence parameter was adjusted to account for the background fluorescence generated by variable Srx concentrations.

(B) Pre-steady state kinetics for the rapid dilution or (C) association of a $Tsa1_{SH}$ (2.5 µM final concentration) and variable Srx mixture in solution monitored by Trp fluorescence. The kinetics series is shown for wild-type $Tsa1_{SH}$. As expected, the decreasing traces for dissociation are increasing for association. The data are globally fitted (red lines) using the Kintek Explorer software using the model and equation shown in (A). The four rate constants and the fluorescence intensity factors for Tsa1•Srx and Tsa1•Srx* were adjusted, in addition to the offset fluorescence background. Due to the complexity of the model, some parameters (the Tsa1•Srx* intensity factor q and k_2) were dependent and could not be defined. The adjusted rate constants are reported in Table S2.

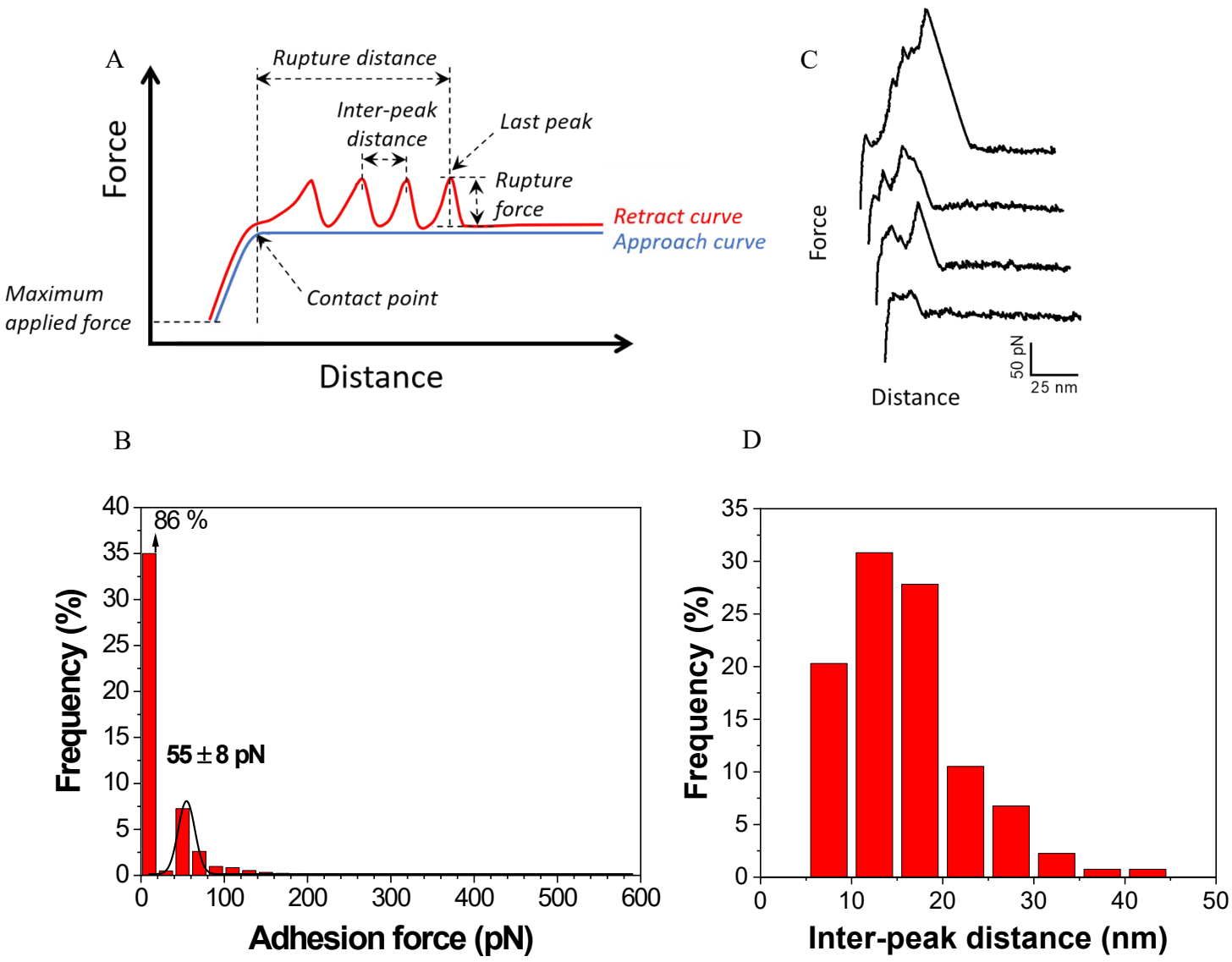

Fig. S8. (A) Definition of parameters used to describe the multipeak force-distance signatures. (B) Adhesion force histogram of Srx attached to the AFM tip binding to Tsa_{SO2} obtained for a contact time set to 0 ms (n=3072 force curves). (C) Examples of hybrid force-distance profiles appearing as a combination of the signatures shown in Fig 4h. (D) Histogram of the interpeak distance distribution measured on the multipeaks force signature (n= 133 peaks from 81 curves).

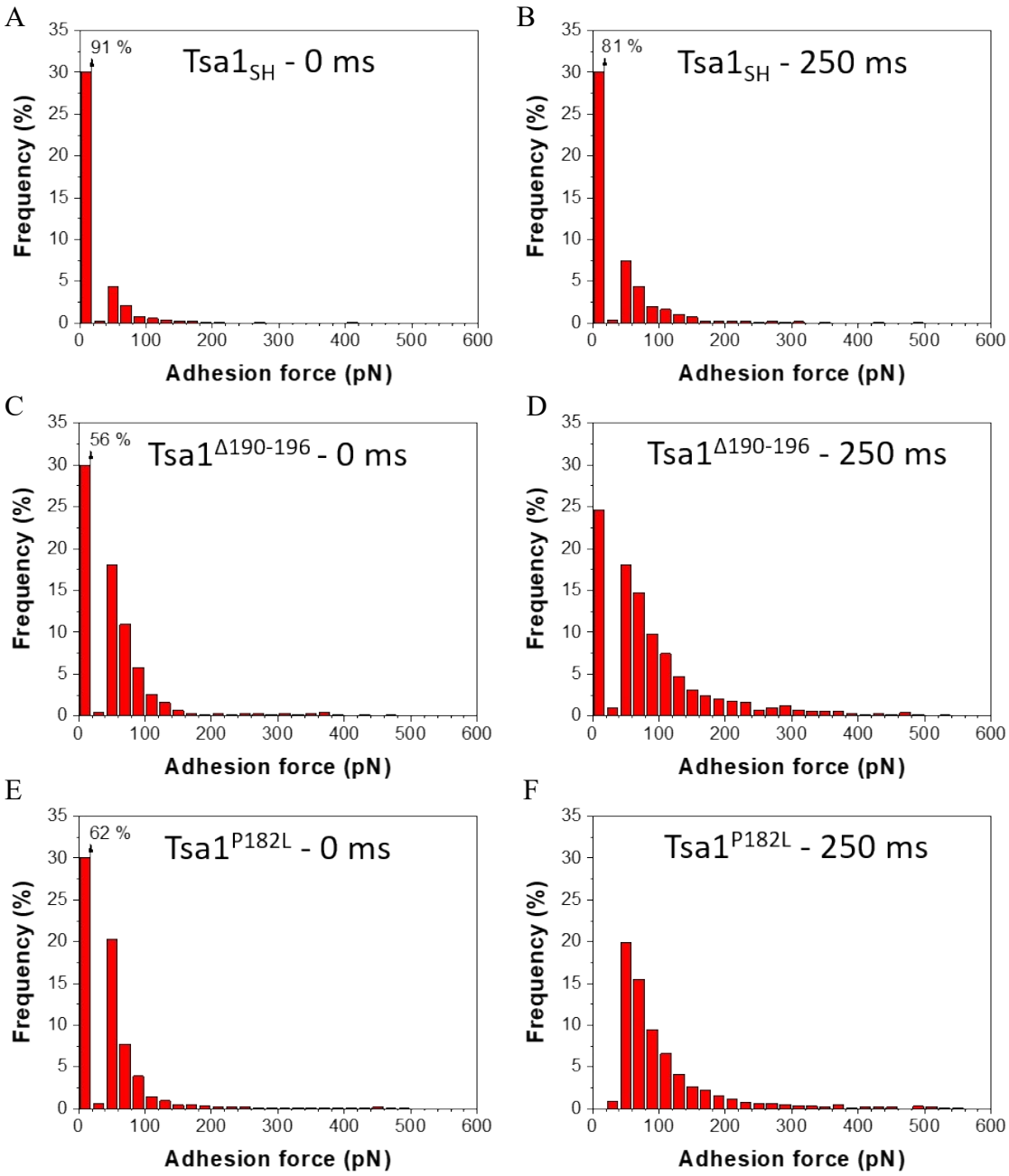

Fig. S9. AFM single-molecule force spectroscopy measurements of Srx binding to wild-type and mutant Tsa1 decamers.

Adhesion force histograms of Srx attached to the AFM tip binding to wild-type (A,B), Δ190-196 (C,D) and P182L (E,F) $Tsa1_{SH}$ obtained for a contact time set to 0 ms (A,C,E) and 250 ms (B,D,F). Each histogram has been built from 3072 force curves obtained from 3 independent experiments using different functionalized tips.

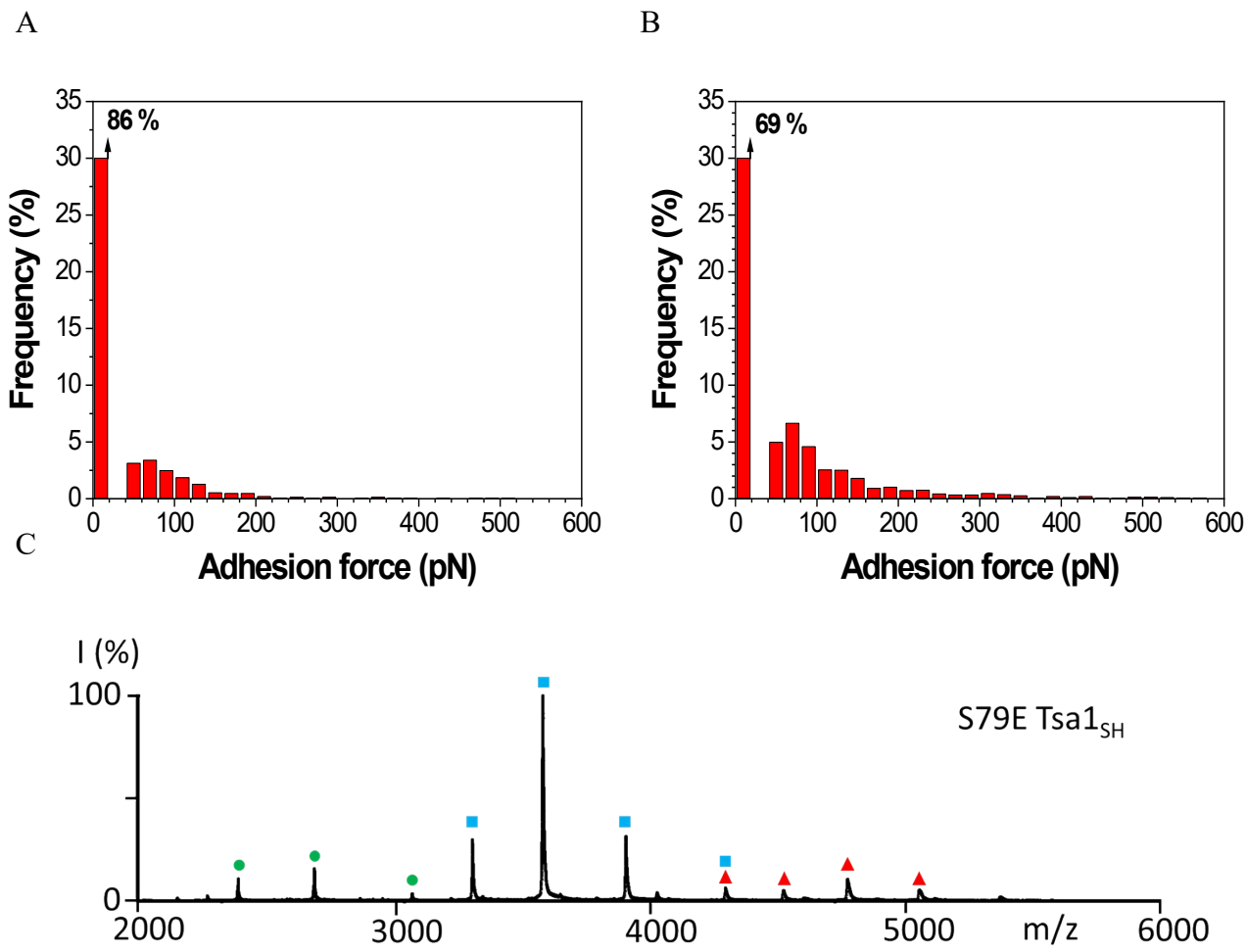

Fig. S10. Adhesion force histograms of $Srx^{C48S\ C84A\ C106V}$ attached to the AFM tip binding to $Tsa1_{SS}$ (A) and wild-type Srx to $Tsa1^{S79E}$ (B) obtained for a contact time between the 2 proteins set to 250 ms. (C) Electrospray ionization native mass spectra of $Tsa1^{S79E}$ C171A mutant (1 µM in decamer) in the reduced state, obtained in native conditions in the gas phase at Vc=80 V showing a main species corresponding to the dimer (🕘; 42,938 ± 1 Da/42,937 Da), and minor species corresponding to the monomer (●; 21,468.6 ± 1.2 Da/21,468.5 Da) and the tetramer (①; 85,885 ± 8 Da/85,874 Da) (experimental/theoretical mass for each form). Formation of unspecific disulfide bonds between dimers was avoided by mutating C171 into Ala. The $Tsa1^{S79E\ C171A}$ mutant, and by extension the $Tsa1^{S79E}$ mutant exist mostly as a dimer.

Table S1. List of mutants and redox forms of Tsa1 and Srx used in the study.

Protein	Mutation	Property	Use
Tsa1	wild-type		$Tsa1_{SH}$, $Tsa1_{SS}$, $Tsa1_{SO2}$
	C171A	Substitution of Cys C_R to Ala	Tsa1-SS-Srx
			Non-covalent interaction experiments as:
	P182L	Mutations conferring increased	$Tsa1_{SH}$
	Δ190-196	flexibility of the C-terminal tail – mutants that do not hyperoxidize	$Tsa1_{SH}$
	S79E	Mutation destabilizing interface A of the decamer	$Tsa1_{SH}$
Srx	wild-type		Non-covalent interaction experiments
	L77R	Mutation of the backside interface of Srx – affects the Tsa1/Srx interaction	Non-covalent interaction experiments
	$Srx^{C48A\ C106V}$	Mutant retaining only Srx catalytic Cys	Tsa1-SS-Srx
	$Srx^{C48S\ C84A\ C106V}$	All Srx Cys substituted	Used to prove the observation of disulfide bond formation with Tsa1

Table S2. Rate constants for dissociation and association kinetics of wild-type and mutant $Tsa1_{SH}$ in complex with Srx.

$Tsa1_{SH}$		k_1 ($M^{-1}s^{-1}$)	k_{-1} (s^{-1})	k_{-2} (s^{-1})
Wild-type	Dissociation	1.0 ± 0.1	18.8 ± 2.8	2.2 ± 1.1
	Association	0.7 ± 0.2	32 ± 8	6.6 ± 1.5
P182L	Dissociation	2.3 ± 1.0	11.8 ± 3.0	1.6 ± 0.2
	Association	1.4 ± 0.02	9.8 ± 1.1	4.5 ± 0.02
Δ190-196	Dissociation	1.4 ± 0.5	7.5 ± 2.2	1.0 ± 0.2
	Association	0.9 ± 0.1	7.6 ± 0.3	2.4 ± 0.3

Rate constants are reported as the mean value obtained from at least 2 independent experiments performed on distinct protein productions ± s.d or range.